

# Mesoporous molecular sieve Al-MCM-41 as a novel catalyst for vapor-phase Beckmann rearrangement of cyclohexanone oxime

An-Nan. Ko \*, Chia-Chun Hung, Chih-Wei Chen and Kuang-Hao Ouyang

*Department of Chemistry, Tunghai University, Taichung, Taiwan, ROC*

Received 9 August 2000; accepted 6 November 2000

Vapor-phase Beckmann rearrangement of cyclohexanone oxime to  $\epsilon$ -caprolactam has been studied at 1 atm and 300–400 °C using mesoporous molecular sieve Al-MCM-41. Benzene and ethanol are utilized as solvents for cyclohexanone oxime. Increasing the reaction temperature enhances the catalyst activity and stability whereas  $\epsilon$ -caprolactam selectivity varies only slightly. Ethanol exhibits much better catalytic results than benzene. Excellent catalyst performance is attained at 1 atm, 400 °C and  $W/F_C$  149.2 g h/mol by using ethanol in the feed; the cyclohexanone oxime conversion and the  $\epsilon$ -caprolactam selectivity remain higher than 99 and 90%, respectively, during at least 1200 h process time. The highly efficient catalysis on Al-MCM-41 is attributed to its large surface area, uniform mesopores as well as the weak and medium acidity.

**KEY WORDS:** Al-MCM-41; Beckmann rearrangement;  $\epsilon$ -caprolactam; cyclohexanone oxime; solid acid

## 1. Introduction

$\epsilon$ -caprolactam ( $\epsilon$ -C) is an important raw material for the manufacture of synthetic fibers. It is normally made in the liquid phase via Beckmann rearrangement of cyclohexanone oxime (CHO) using concentrated sulfuric acid as the catalyst. Despite its high selectivity, this homogeneous catalyzed process suffers from the large amount of ammonium sulfate produced and corrosion problems. Consequently, the vapor-phase reaction over heterogeneous catalysts has drawn much attention during the past three decades [1]. Investigations were performed over silica–alumina [2], boria or other species supported on alumina [3,4], boria supported on zirconia [5] and several zeolites including HY [6,7], Pd/Y [6], ZSM-5 [8], [B]-ZSM-5 [9], Beta [10,11], [Al]- and [B]-Beta [12], and mesoporous molecular sieves [13].

In the reaction of CHO over  $B_2O_3/Al_2O_3$ , the activity diminished with process time, whereas the  $\epsilon$ -C selectivity remained constant during the first five hours. The catalyst decay was attributed to the coke formed on the surface and the  $\epsilon$ -C selectivity was associated with the concentration of intermediate strength acid sites [4].  $B_2O_3/ZrO_2$  was reported to be highly active and selective for the synthesis of  $\epsilon$ -C at 300–320 °C during 8 h process time; the  $\epsilon$ -C yield is parallel to the number of intermediate strong acid sites [5]. Over ultrastable HY zeolite, different decay models were discussed and the kinetic parameters were calculated according to the time-on-stream theory [7]. For the reaction over a boron-MFI zeolite, reducing the temperature and the pressure increased the  $\epsilon$ -C selectivity, but shortened the catalyst lifetime. Addition of water up to 6 mol per mol CHO resulted in an increase of catalyst lifetime [9]. Similar effects were observed on aluminum- or boron-containing Beta ze-

olites. Although both catalysts exhibited very high initial activity, rapid deactivation was observed and thus catalyst regeneration was necessary for industrial application [12]. For the reaction over H-MCM-41 and H-FSH-16 during 6 h process time, H-MCM-41 exhibited better performance with 1-hexanol as diluent [13]. So far, therefore, the major drawback of this reaction over solid acid catalyst lies in the fast rate of deactivation [9].

The mesoporous molecular sieve Al-MCM-41 was recently developed and was reported to exhibit large surface area, uniform pores with diameters 20–100 Å, as well as weak and intermediate acidity [14–16]. Such a catalyst has been applied in many acid-catalyzed reactions, especially in the fields of oil refining, petrochemistry and the synthesis of chemicals and fine chemicals [17–19]. In this work, the Beckmann rearrangement of CHO to  $\epsilon$ -C is studied using Al-MCM-41 as catalyst. CHO dissolved in benzene or ethanol are chosen as the feed. Their catalytic performances are compared and correlated to catalyst properties. Here novel catalytic results are attained by using a feed of CHO in ethanol; it exhibits much better catalytic results, viz. very high CHO conversion (>99%),  $\epsilon$ -C selectivity (>90%), and excellent catalyst stability during at least 1200 h process time.

## 2. Experimental

### 2.1. Synthesis of Al-MCM-41

Al-MCM-41 was synthesized similar to methods described in the literature [16]. Solutions A and B were prepared by dissolving 36 g cetyltrimethylammonium bromide (99%, Aldrich) in 264 g water and 0.6 g sodium aluminate (RDH) in 30 g water, respectively. Then 53 g sodium silicate

\* To whom correspondence should be addressed.

(RDH) and solution B were added with rigorous stirring into solution A. Finally, 60 g 1.1 M  $\text{H}_2\text{SO}_4$  was added and stirred well to obtain the pH value 9–10 of the resultant solution. The gel was crystallized at 100 °C for 48 h in an autoclave. The crystals were washed with water and dried at 110 °C for 12 h. The as-synthesized sample was calcined at 540 °C for 6 h.

## 2.2. Catalyst characterization

The Si/Al mol ratio of the sample was obtained with an ICP-AES (Allied Analytical ICAP 2000). The powder X-ray diffraction patterns of samples were measured with a XRD spectrometer (Shimadzu XD-5). The BET surface area of the Al-MCM-41 catalyst was measured with a sorption analyzer (Quantasorb). The pore size distribution and  $\text{N}_2$  adsorption isotherm of the sample were also determined (Micromeritics ASAP 2000). The catalyst acidity was obtained by temperature-programmed desorption of ammonia. Before adsorption, the catalyst sample (0.1 g) was heated under helium flow (40 ml/min NTP) with a rate of 10 °C/min from 110 to 540 °C to remove water from the sample and then the sample was cooled to room temperature. Measured pulses of ammonia (pulse volume, 0.5 ml NTP) were injected into helium gas and carried through the sample until adsorption saturated. The temperature was then increased to 110 °C and it was kept there for 2 h to remove the physisorbed ammonia. Finally, the system was heated from 110 to 540 °C at 10 °C/min and kept at 540 °C for 35 min. The TPD graphs were obtained by monitoring the desorbed gas with a thermal conductivity detector. For the calcined Al-MCM-41 sample adsorbed with pyridine vapor, it was successively evacuated at 200, 300 and 400 °C. The corresponding IR spectra were recorded at 20 °C with an FT-IR spectrometer (Perkin-Elmer 2000) using a MCT mid-IR detector. The  $^{27}\text{Al}$  and  $^{29}\text{Si}$  MAS NMR spectra were determined for the Al-MCM-41 catalysts (Bruker MSL 200 MHz).

## 2.3. Catalytic reaction

The catalytic reactions were carried out in a fixed-bed, integral-flow reactor at 1 atm and in the range of 300–400 °C. Prior to the reaction, the catalyst was activated with flowing dry air (60 ml/min) at 400 °C for 2 h and then cooled to the reaction temperature with nitrogen gas (99.99%, 60 ml/min). The feed was prepared by dissolving CHO in benzene or ethanol (1 mol/l). It was injected via a microfeeder (Stoelting) into the reactor (1 cm I.D.  $\times$  34 cm), containing 0.038–0.30 g Al-MCM-41. Nitrogen was used as the carrier gas (60 ml/min). The value of  $W/F_C$  referred to the weight of catalyst per unit feed rate of CHO. The effluents were collected with a condenser. The liquid products were identified with a GC-MS (HP 5989 B) and were periodically analyzed with a GC (China Chromatography Co.) fitted with a FID and a megabore column DB-1 (J&W, 0.544 mm  $\times$  30 m).

## 3. Results and discussion

### 3.1. Catalyst properties

The ICP-AES analysis of Al-MCM-41 gives a Si/Al mol ratio of 25.0 in the bulk sample. Figure 1 shows the powder X-ray diffraction patterns of the Al-MCM-41 materials. The as-synthesized sample exhibits three peaks, viz. a strong peak at a  $d$ -spacing of 43.3 Å and two small peaks at 24.3 and 21.0 Å. After calcination, a decrease of  $d$ -spacing was observed for all these peaks due to the removal of organic template; the corresponding values are 37.1, 21.7 and 18.9 Å. However, the (110) and (200) peak intensities slightly increase. These well-defined patterns are characteristic of the Al-MCM-41 structure [20] and can be indexed on a hexagonal lattice with unit cell parameter  $a_0 \approx 45.4$  Å [21]. The sharp and intense (100) peak appears in both samples.

According to the  $\text{N}_2$  adsorption isotherm of the calcined sample [19], a hysteresis loop in the region of  $P/P_0$  above 0.4 is attributed to the capillary condensation in the mesopores. Two peaks appear in the pore size distribution, viz. the main peak at 20–30 Å and the small one at 30–40 Å. In addition, the BET surface area and the pore volume are 1014  $\text{m}^2/\text{g}$  and 1.45 ml/g, respectively. Figure 2 shows the  $^{27}\text{Al}$  and  $^{29}\text{Si}$  MAS NMR spectra of the various samples of Al-MCM-41. In the case of the as-synthesized sample (figure 2(A), curve (a)), the peak at 53 ppm corresponds to tetrahedral-coordinated structural

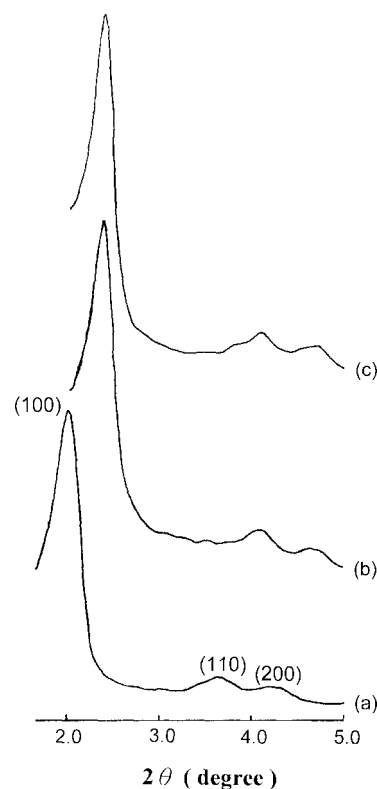


Figure 1. Powder XRD patterns of Al-MCM-41: (a) as-synthesized, (b) calcined and (c) after reaction.

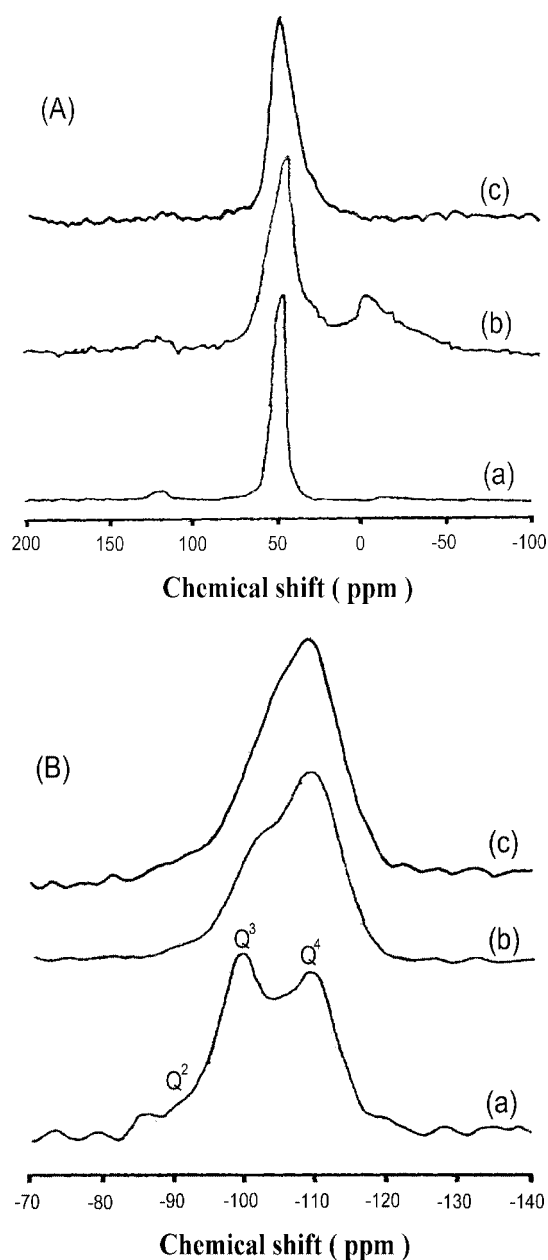


Figure 2. The MAS NMR spectra of Al-MCM-41: (A)  $^{27}\text{Al}$  and (B)  $^{29}\text{Si}$ ; (a) as-synthesized, (b) calcined and (c) after reaction.

aluminum. A new peak at 0 ppm appears after calcination (figure 2(A), curve (b)) that is attributed to the aluminum expelled from the Al-MCM-41 structure [22]. The environment of silicon in the skeletal structure of molecular sieves is usually written as  $\text{Q}^n$  to represent  $\text{Si}(\text{OSi})_n(\text{OH})_{4-n}$ . For the as-synthesized Al-MCM-41, three resonances ( $\text{Q}^2$ – $\text{Q}^4$ ) are observed at  $-92$ ,  $-101$  and  $-110$  ppm, respectively (figure 2(B), curve (a)) [23]. Calcination results in the apparent decrease of  $\text{Q}^3$  peak intensity due to dehydration occurring on the surface of  $\text{Si-OH}$ ; the spectrum is similar to that of amorphous silica (figure 2(B), curve (b)).

Figure 3 shows the temperature-programmed desorption profiles of ammonia from the Al-MCM-41 sample. A broad peak occurs that indicates the broad distribution of weak and

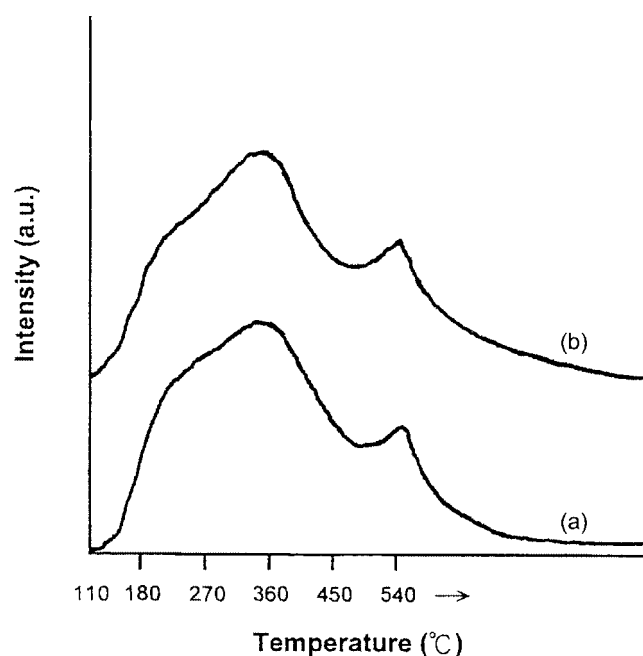


Figure 3.  $\text{NH}_3$ -TPD profiles from Al-MCM-41: (a) calcined and (b) after reaction.

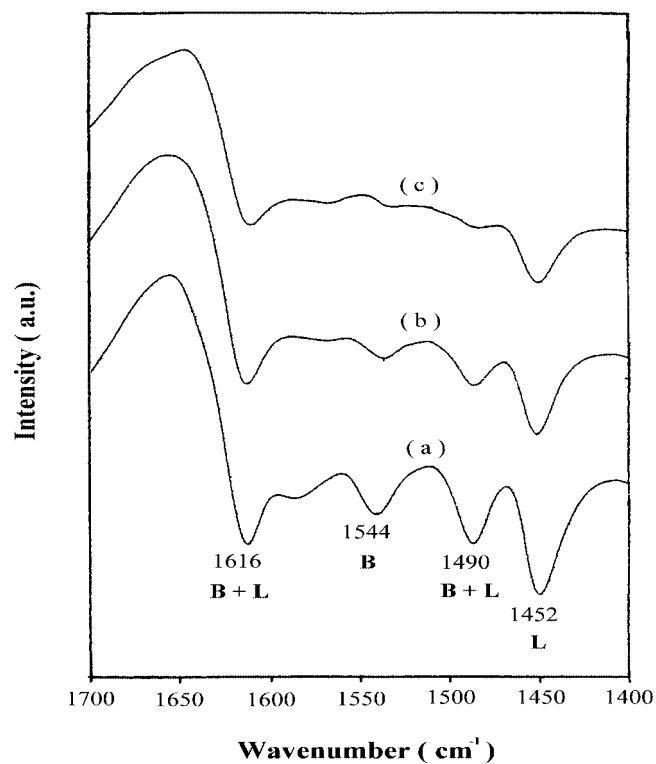


Figure 4. FT-IR spectra of calcined Al-MCM-41 adsorbed with pyridine, followed by successive evacuation at (a) 200, (b) 300 and (c) 400  $^{\circ}\text{C}$ . B: Brønsted acid sites and L: Lewis acid sites.

medium strength acid sites. Figure 4 illustrates the FT-IR spectrum of calcined Al-MCM-41 adsorbed with pyridine. The peaks at ca. 1452 and 1544  $\text{cm}^{-1}$  correspond to Lewis and Brønsted acid sites, respectively [24]. The sample contains a larger amount of Lewis acid sites than of Brønsted

Table 1  
Catalytic activities and product selectivities over Al-MCM-41.<sup>a</sup>

Solvent	Reaction temperature (°C)	Process time (h)	CHO conversion (mol%)	Product selectivity (mol%) <sup>b</sup>					
				$\varepsilon$ -C	HEN	HAN	CHA	CHE	AN
C <sub>6</sub> H <sub>6</sub>	300	4	27.1	79.9	0	11.8	4.98	3.32	0
C <sub>6</sub> H <sub>6</sub>	350	4	78.7	70.8	0.47	18.5	5.13	3.90	1.20
C <sub>6</sub> H <sub>6</sub>	370	4	92.2	73.0	0	18.2	4.56	3.40	0.84
C <sub>6</sub> H <sub>6</sub>	400	4	100	74.6	0.98	13.4	4.91	3.47	2.64
C <sub>2</sub> H <sub>5</sub> OH	350	4	94.8	83.2	0	10.3	3.57	1.87	1.06
C <sub>2</sub> H <sub>5</sub> OH	350	26	63.9	90.5	0	4.17	4.15	1.18	0
C <sub>2</sub> H <sub>5</sub> OH	370	4	99.3	83.0	0	10.9	3.39	1.71	1.00
C <sub>2</sub> H <sub>5</sub> OH	370	26	91.7	89.3	0	5.91	3.42	1.37	0
C <sub>2</sub> H <sub>5</sub> OH	385	4	100	83.9	0.65	8.60	3.98	1.97	0.90
C <sub>2</sub> H <sub>5</sub> OH	385	26	100	87.2	0.67	5.69	4.24	1.71	0.49
C <sub>2</sub> H <sub>5</sub> OH	400	4	100	90.5	1.70	3.57	3.21	0.74	0.28
C <sub>2</sub> H <sub>5</sub> OH	400	26	100	91.0	2.65	2.64	2.70	0.72	0.29

<sup>a</sup> Reaction conditions: 1 atm,  $W/F_C$  74.6 g h/mol, 1 mol CHO/l solvent, N<sub>2</sub> flow rate 3.6 l/h.

<sup>b</sup> CHO = cyclohexanone oxime,  $\varepsilon$ -C =  $\varepsilon$ -caprolactam, HEN = 5-hexenenitrile, HAN = hexanenitrile, CHA = cyclohexanone, CHE = cyclohexen-1-one, AN = aniline.

acid sites. As the evacuated temperature increased from 200 to 400 °C, most of the Brønsted acid sites are lost, whereas a significant amount of Lewis acid sites are still present.

### 3.2. Catalytic reactions

In the Beckmann rearrangement of CHO over Al-MCM-41,  $\varepsilon$ -C is the major product and the side products include cyclohexanone (CHA), cyclohexen-1-one (CHE), hexanenitrile (HAN), 5-hexenenitrile (HEN) and aniline (AN) in accordance with the literature [9,13]. The CHO conversion and the product selectivity are calculated with respect to the moles of CHO converted. Benzene or ethanol is utilized as a solvent for CHO in the feed. With pure benzene over Al-MCM-41 no reaction took place, whereas ethylene, diethyl ether and water were produced by feeding pure ethanol.

#### 3.2.1. Effect of reaction temperature

The influence of temperature on the catalytic reactions was studied in the range 300–400 °C. Table 1 shows the dependence of catalytic activity and product selectivity on the temperature. With CHO/C<sub>6</sub>H<sub>6</sub> as feed, the CHO conversion increases remarkably with temperature from 300 to 400 °C at 4 h reaction whereas the  $\varepsilon$ -C selectivity varies only slightly. If ethanol is used as solvent, the catalytic activities at both 4 and 26 h reaction are also parallel to the reaction temperature between 350 and 400 °C. Furthermore, much higher  $\varepsilon$ -C selectivity is attained with concomitant decrease of hexanenitrile selectivity. At temperature higher than 370 °C, the product selectivities are practical constant which suggests the high stability of  $\varepsilon$ -C without successive reactions to yield side products. These results are consistent with literature reports [9].

#### 3.2.2. Effect of contact time

Table 2 shows the influence of contact time on the catalytic results at short process time of 15 min using the feed

Table 2  
Influence of contact time on the CHO conversion and the product yield.<sup>a</sup>

$W/F_C$ (g h/mol)	Conversion (mol%)	Product yield (mol%)					
		$\varepsilon$ -C	HEN	HAN	CHA	CHE	AN
2.33	51.2	36.4	0.42	9.30	2.87	1.17	1.04
4.67	73.1	49.9	0.60	14.9	4.38	2.27	1.05
9.33	99.0	70.2	0.76	17.0	5.61	3.32	2.11
18.1	98.1	66.8	1.76	17.9	5.66	3.73	2.25
37.3	100	67.5	1.23	18.6	5.61	3.76	3.30
74.6	100	65.9	1.91	16.1	8.14	3.08	4.87

<sup>a</sup> Reaction conditions: 400 °C, 1 atm, 1 mol CHO/l benzene, N<sub>2</sub> flow rate 3.6 l/h.

CHO/C<sub>6</sub>H<sub>6</sub>. As the contact time increases from  $W/F_C$  2.33 to 9.33 g h/mol, the CHO conversion also increases dramatically from 51.2 to 99.0% and thereafter remains unchanged. Similar trends are observed for the product yields. Figure 5 shows catalytic activities and  $\varepsilon$ -C selectivities at  $W/F_C$  74.6 and 298 g h/mol for CHO/C<sub>6</sub>H<sub>6</sub> reactions over Al-MCM-41 at 400 °C. It takes 11 and 25 h, respectively, for CHO conversions to drop to 70%; the corresponding  $\varepsilon$ -C selectivities are 76 and 81%.

#### 3.2.3. Effect of solvent

Nonpolar benzene and polar ethanol solvents were utilized to investigate their influences on the catalytic activity, the product selectivity and the catalyst stability. Both the CHO conversion and the  $\varepsilon$ -C selectivity are much higher by using ethanol as compared to benzene (table 1). Figure 6 shows the catalytic results as a function of process time by using CHO/ethanol under the reaction conditions of 400 °C and  $W/F_C$  149.2 g h/mol. The results exhibit superior catalytic performance than those of CHO/benzene; the CHO conversions and  $\varepsilon$ -C selectivities are larger than 99 and 90%, respectively, for the process time over 1200 h. This is explained as follows: ethanol dehydrates to ethylene, diethyl ether and water over Al-MCM-41 under the same reaction conditions as confirmed by the blank reaction using only

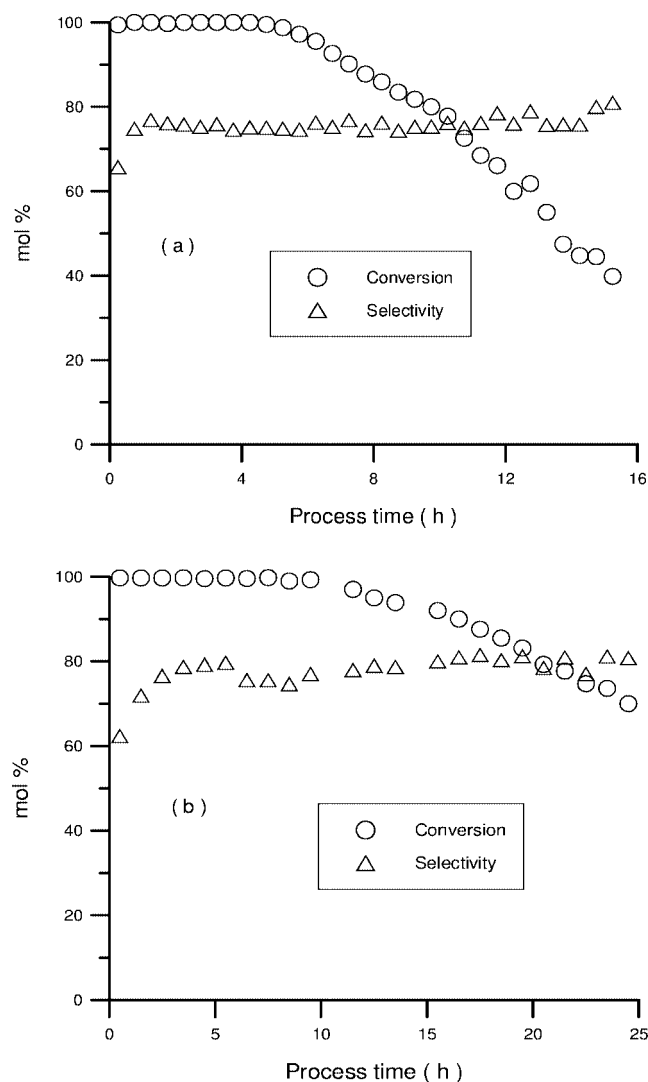


Figure 5. Catalytic results for CHO/C<sub>6</sub>H<sub>6</sub> reactions over Al-MCM-41 at 400 °C,  $W/F_C$  (a) 74.6 and (b) 298 g h/mol.

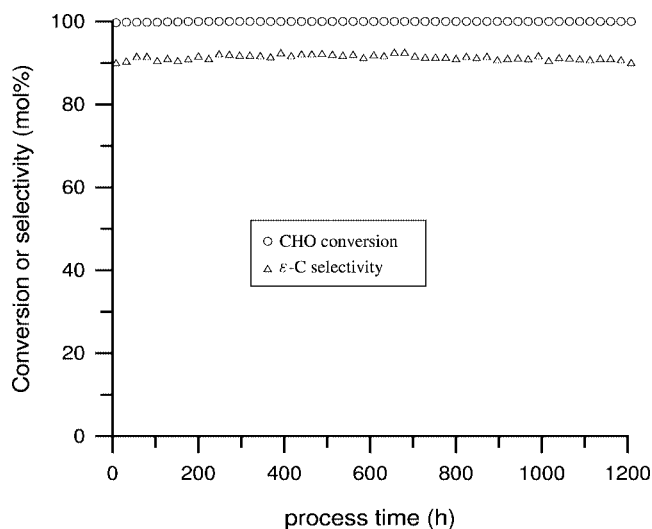


Figure 6. Catalytic results for CHO/C<sub>2</sub>H<sub>5</sub>OH reactions over Al-MCM-41 at 400 °C and  $W/F_C$  149.2 g h/mol.

ethanol in the feed. During the reaction, both ethanol and the continuously produced water suppress the formation of polymers and coke on the catalyst surface. The positive effect of water on preventing deactivation was verified in the CHO reaction using B-MFI zeolites [9]. According to the results shown in figure 5, the catalyst stability enhances greatly with increasing  $W/F_C$  values in the reaction of CHO/C<sub>6</sub>H<sub>6</sub>. Such conclusion can reasonably be extended to the reaction using CHO/C<sub>2</sub>H<sub>5</sub>OH. Accordingly, the catalyst lifetime should also become much longer at  $W/F_C$  298 g h/mol. The extremely high stability of Al-MCM-41 is remarkably better than those of other solid acids where only several days of catalyst lifetime were reported [9]. After the catalytic reaction of 1200 h process time, the used catalyst was characterized with XRD, BET, TPD and MAS NMR in order to investigate its physicochemical properties and thus the possible cause for its excellent catalytic performance. The XRD patterns of the used catalyst are quite similar to those of the fresh catalyst, indicating the retention of crystal structure after reaction (figure 1). Furthermore, a comparison of the ammonia TPD profiles of the fresh and the used catalysts reveals only small variation in their catalyst acidities (figure 3). In addition, no significant difference was observed on the <sup>27</sup>Al and <sup>29</sup>Si NMR spectra of the two catalyst samples (figure 2, curves (b) and (c)). The above results infer that the catalyst properties remain stable during the catalytic reaction. Although the BET surface area decreases from 1014 to 622 m<sup>2</sup> g<sup>-1</sup> after 1200 h reaction, both the catalytic activity and  $\epsilon$ -C selectivity do not decline. It is proposed that the pore blockage, especially at the micropores, results in the decrease of both the surface area and the pore volume whereas the mesopores, being the location of pertinent active sites, remain active during the reaction. In summary, the highly efficient catalysis on Al-MCM-41 is attributed to its uniform mesopores, weak and intermediate acidity as well as the large surface area.

#### 4. Conclusion

In this work, Al-MCM-41 with Si/Al mol ratio of 25.0 exhibits excellent performance in the vapor phase Beckmann rearrangement of cyclohexanone oxime to  $\epsilon$ -caprolactam by using ethanol as solvent. For the reaction at 400 °C, 1 atm and  $W/F_C$  149.2 g h/mol, the CHO conversion and the  $\epsilon$ -C selectivity remain, respectively, higher than 99 and 90% during a process time greater than 1200 h. Consequently, Al-MCM-41 is a potential catalyst for the manufacture of  $\epsilon$ -C from CHO.

#### Acknowledgement

We thank the National Science Council of the Republic of China for financial support (NSC 88-2113-M-029-004). We also thank Professor K.J. Chao and Mr. C.P. Ho of National Tsing Hua University for their comments and assistance in XRD and gas adsorption measurements.

## References

- [1] W.F. Hölderich, in: *Comprehensive Supramolecular Chemistry*, Vol. 7, eds. G. Alberti and T. Bein (Pergamon, New York, 1996).
- [2] O. Immel, H.H. Schwarz, K. Starke and W. Swodenk, *Chem. Inorg. Tech.* 56 (1984) 612.
- [3] BASF, Ger. Patent 1 227 028 (1976).
- [4] T. Curtin, J.B. McMonagle and B.K. Hodnett, *Appl. Catal. A* 93 (1992) 75.
- [5] B.-Q. Xu, S.-B. Cheng, S. Jiang and Q.-M. Zhu, *Appl. Catal. A* 188 (1999) 361.
- [6] J.D. Butler and T.C. Poles, *J. Chem. Soc. Perkin II* (1973) 1262.
- [7] M.C. Burguet, A. Aucejo and A. Corma, *Canad. J. Chem. Eng.* 65 (1987) 944.
- [8] J. Sauer and A. Bleiber, *Catal. Today* 3 (1988) 485.
- [9] J. Roseler, G. Heitmann and W.F. Hölderich, *Appl. Catal. A* 144 (1996) 319.
- [10] E.R. Herrero, O.A. Anunziata, L.B. Pierella and O.A. Orio, *Lat. Am. Appl. Res.* 24 (1994) 195.
- [11] K.-H. Ou-yang and A.-N. Ko, in: *5th Int. Symp. on Heterogeneous Catalysis and Fine Chemicals*, 30 August–3 September 1999, Lyon, France, Book of Abstracts, p. 40.
- [12] G.P. Heitmann, G. Dahlhoff and W.F. Hölderich, *Appl. Catal. A* 185 (1999) 99.
- [13] L.-X. Dai, K. Koyama and T. Tatsumi, *Catal. Lett.* 53 (1998) 211.
- [14] C.T. Kresge, M.E. Leonowicz, W.J. Roth, J.C. Vartuli and J.S. Beck, *Nature* 359 (1992) 710.
- [15] X.S. Zhao, G.Q. (Max) Lu and G.J. Millar, *Ind. Eng. Chem. Res.* 35 (1996) 2075.
- [16] H.P. Lin, S. Cheng and C.-Y. Mou, *J. Chin. Chem. Soc.* 43 (1996) 375.
- [17] A. Corma, A. Martinez, V. Martinez-Soria and J.B. Monton, *J. Catal.* 153 (1995) 25.
- [18] K. Chaudhari, T.K. Das, A.J. Chandwadkar and S. Sivasanker, *J. Catal.* 186 (1999) 81.
- [19] L.-W. Chen, C.-Y. Chou and A.-N. Ko, *Appl. Catal. A* 178 (1999) L1.
- [20] C.-Y. Chen, H.-X. Li and M.E. Davis, *Micropor. Mater.* 2 (1993) 17.
- [21] J.S. Beck, J.C. Vartuli, W.J. Roth, M.E. Leonowicz, C.T. Kresge, K.D. Schmitt, T.U. Chu, D.H. Olsen, E.W. Sheppard, S.B. McCullen, J.B. Higgins and J.L. Schlenker, *J. Am. Chem. Soc.* 114 (1992) 10834.
- [22] C.-F. Cheng and J. Klinowski, *J. Chem. Soc. Faraday Trans.* 92 (1996) 289.
- [23] A. Liepold, K. Roos, W. Reschetilowski, A.P. Esculcas, J. Rocha, A. Philippou and M.W. Anderson, *J. Chem. Soc. Faraday Trans.* 92 (1996) 4623.
- [24] E.P. Parry, *J. Catal.* 2 (1963) 371.